Role of extracellular histones in the cardiomyopathy of sepsis

Miriam Kalbitz,*[,†] Jamison J. Grailer,* Fatemeh Fattahi,* Lawrence Jajou,* Todd J. Herron,[‡] Katherine F. Campbell,[‡] Firas S. Zetoune,* Markus Bosmann,[§,¶] J. Vidya Sarma,* Markus Huber-Lang,[†] Florian Gebhard,[†] Randall Loaiza,[‡] Hector H. Valdivia,[‡] José Jalife,[‡] Mark W. Russell,[‖] and Peter A. Ward*[,1]

*Department of Pathology and [‖]Department of Pediatrics and Communicable Diseases, University of Michigan Medical School, Ann Arbor, Michigan, USA; [†]Department of Orthopaedic Trauma, Hand, Plastic and Reconstructive Surgery, University Hospital of Ulm, Ulm, Germany; [‡]Center for Arrhythmia Research, University of Michigan, Ann Arbor, Michigan, USA; and [§]Center for Thrombosis and Hemostasis and [¶]Department of Hematology, Oncology and Pneumology, University Medical Center, Mainz, Germany

ABSTRACT   The purpose of this study was to define the relationship in polymicrobial sepsis (in adult male C57BL/6 mice) between heart dysfunction and the appearance in plasma of extracellular histones. Procedures included induction of sepsis by cecal ligation and puncture and measurement of heart function using echocardiogram/Doppler parameters. We assessed the ability of histones to cause disequilibrium in the redox status and intracellular $[Ca^{2+}]_i$ levels in cardiomyocytes (CMs) (from mice and rats). We also studied the ability of histones to disturb both functional and electrical responses of hearts perfused with histones. Main findings revealed that extracellular histones appearing in septic plasma required C5a receptors, polymorphonuclear leukocytes (PMNs), and the Nacht-, LRR-, and PYD-domains–containing protein 3 (NLRP3) inflammasome. *In vitro* exposure of CMs to histones caused loss of homeostasis of the redox system and in $[Ca^{2+}]_i$, as well as defects in mitochondrial function. Perfusion of hearts with histones caused electrical and functional dysfunction. Finally, *in vivo* neutralization of histones in septic mice markedly reduced the parameters of heart dysfunction. Histones caused dysfunction in hearts during polymicrobial sepsis. These events could be attenuated by histone neutralization, suggesting that histones may be targets in the setting of sepsis to reduce cardiac dysfunction.—Kalbitz, M., Grailer, J. J., Fattahi, F., Jajou, L., Herron, T. J., Campbell, K. F., Zetoune, F. S., Bosmann, M., Sarma, J. V., Huber-Lang, M., Gebhard, F., Loaiza, R., Valdivia, H. H., Jalife, J., Russell, M. W., Ward, P. A. Role of extracellular histones in the cardiomyopathy of sepsis. *FASEB J.* 29, 2185–2193 (2015). www.fasebj.org

Key Words: complement · NLRP3 inflammasome · cardiomyocytes · echocardiogram/Doppler · polymicrobial sepsis

Myocardial dysfunction is observed in 50% of patients diagnosed with sepsis (1) and is correlated with mortality rates as high as 70% (2). Defects in cardiac performance during sepsis appear to be reversible in patients who survive sepsis (3, 4). Products known as damage-associated molecular patterns (DAMPs) (5) are released from cells during sepsis or are actively secreted as endogenous alarm signals to warn the host of danger (6). Extracellular histones function as endogenous DAMPs, which may interact with toll-like receptor (TLR) 2 and TLR4 on a variety of different cell types, including cardiomyocytes (CMs) (7–9). Circulating extracellular histones in plasma have been detected in patients in septic shock, and it has been shown that extracellular histones released in response to experimental sepsis contribute to endothelial dysfunction, organ failure, and death (10–12). Histones also play important roles in sterile sepsis that occur after chemically induced acute liver injury, hemorrhagic shock, or ischemia-reperfusion injury (8, 9). Histones have been detected in blood from baboons challenged with live *Escherichia coli* (10). Neutralizing antibodies to histones reduced mortality in mice infused with TNF or LPS, as well as in mice with polymicrobial sepsis (10), suggesting that extracellular histones are major mediators of death in sepsis. In the setting of trauma, circulating histones were detected in plasma immediately after nonthoracic blunt trauma in humans, accompanied by acute lung injury (ALI) (12, 13). In rodents with C5a-induced ALI, extracellular histones appeared in broncho-alveolar lavage fluids (BALF), as well as in BALF from humans with ALI. Histone appearance was complement and polymorphonuclear leukocyte (PMN)-dependent (14). Histone administration into mouse airways caused intense inflammation, damage of alveolar epithelial cells, release of cytokines/chemokines, and severe disturbances in gas exchange in lungs together with prominent thrombi in pulmonary veins. Using a mAb with neutralizing activity for

[1] Correspondence: University of Michigan Medical School, Department of Pathology, 1301 Catherine Rd., 7520 MSRB I, Box 5602, Ann Arbor, MI 48109-5602. E-mail: pward@umich.edu

extracellular histones, these defects were markedly attenuated (14). The current report suggests that extracellular histones act as DAMPs and are linked to development of cardiac dysfunction during sepsis. Use of neutralizing mAbs to histones was found to be heart protective.

MATERIALS AND METHODS

Animals and anesthesia

All procedures conformed to the *Guide of Care and Use of Laboratory Animals* published by the U.S. National Institutes of Health. The study was approved by the University Committee on Use and Care of Animals and performed according to appropriate guidelines. Specific pathogen-free male Sprague-Dawley rats (300–350 g; Harlan Laboratories, Indianapolis, IN, USA) and male C57BL/6 mice (6–10 weeks, 20–30 g; The Jackson Laboratory, Bar Harbor, ME, USA) were anesthetized using the combination of ketamine (Hospira, Lake Forest, IL, USA) and xylazine (Lloyd Laboratories, Shenandoah, IA, USA) intraperitoneally. $NLRP3^{-/-}$, caspase $1^{-/-}$, TLR $2^{-/-}$, and TLR $4^{-/-}$ mice were purchased from The Jackson Laboratory. $C5aR1^{-/-}$ and $C5aR2^{-/-}$ mice were generated in our own laboratories, as described earlier (15, 16). The number of mice used in each experiment is detailed in legends to figures.

Reagents

The following reagents were used: neutralizing histone antibody (clone BWA3) (17) and mouse IgGk isotype matched antibody (BioLegend, San Diego, CA, USA); purified histones from calf thymus and chemicals used for preparation of solutions for CM isolation were purchased from Sigma-Aldrich (St. Louis MO, USA). Endotoxin contamination of the histone preparations was <0.02 EU/mg (LAL assay; Lonza, Allendale, NJ, USA).

Experimental sepsis

Sepsis was induced by the cecal ligation and puncture (CLP) procedure as described previously in both rats and mice (18, 19). Sham animals underwent the same procedure, including manipulation of the bowel in the absence of cecal ligation and puncture. All animals (sham and CLP) received fluid resuscitation (1.5 ml lactated Ringers, given subcutaneously in the nuchal region). The animals were euthanized at times indicated after CLP.

Isolation of CMs

The isolation of adult rat or mouse CMs was performed as previously described, using a Langendorff perfusion system (20, 21). The hearts were retrograde perfused with enzyme solution, according to manufacturer's directions (Liberase; Hoffmann-La Roche, Mannheim, Germany). Following digestion, the heart was detached from the Langendorff apparatus, atria and vessels were removed, and the ventricles were cut into small pieces, which were

---

(*continued from previous page*)
FCCP, carbonyl cyanide 4-(trifluoromethoxy) phenylhydrazone; LV, left ventricle; NET, neutrophil extracellular trap; NLRP3, Nacht-, LRR-, and PYD-domains-containing protein 3; PMN, polymorphonuclear leukocytes; ROS, reactive oxygen species; TLR, toll-like receptor; TMRE, tetramethylrhodamine, ethyl ester; WT, wild-type

gently triturated with a plastic transfer pipette. After isolation of the CMs, the Ca^{2+} concentration in the buffer fluid was gradually increased (to 1.8 mM), and the cells were cultured in M199 medium with 1% insulin-transferrin-selenium-X (Gibco; Life Technologies, Carlsbad, CA, USA) and antibiotic-antimycotic (Invitrogen, Carlsbad, CA, USA). In some cases, anti-histone neutralizing antibody or an irrelevant isotype control antibody was administered intravenously (400 μg/mouse) at the time of CLP. In some cases, neutrophils were depleted by intraperitoneal injection of 150 μg anti-Ly6G (clone 1A8, or isotype control antibody, both from BioLegend, San Diego, CA, USA) 12 hours prior to CLP.

Histone ELISA

Histones in mouse plasma were measured by using a cell death detection ELISA kit that detects all histones (Hoffmann-La Roche, Indianapolis, IN, USA). A histone mixture (containing H2, H2A, H2B, H3, and H4) was used to establish a standard curve, as previously described (14).

Measurement of $[Ca^{2+}]_i$ and reactive oxygen species

Intracellular Ca^{2+} in CMs was measured by flow cytometry using Fluo3 AM, whereas intracellular cytosolic reaction oxygen species (ROS) was measured using CellROX Deep Red (Invitrogen, Life Technologies, Carlsbad, CA, USA) according to manufacturer's directions. A minimum of 10,000 events was analyzed on a BD LSR II flow cytometer (BD Biosciences, San Jose, CA, USA) with Diva Software (San Jose, CA, USA). Data were analyzed with FlowJo Software 7.6.4 (Ashland, CA, USA).

Calcium currents in rat CMs

CM calcium currents were measured as previously described (22).

Transthoracic echocardiography in mice

Echocardiograms were performed as previously described (23). All echocardiograms were performed by a registered echocardiographer who was blinded to experiment details. Mice were weighed and anesthetized with inhaled isoflurane. Imaging was performed according to the recommendations of the American Society of Echocardiography using Vevo 770 Microimaging system (Visualsonics Inc) equipped with an RMV707B (15–45 MHz) transducer. Left ventricular area and left ventricular length were measured from the parasternal long axis view and used to calculate the left ventricular end systolic and diastolic volumes as follows:

$$V = 4/3\pi \times \frac{\text{length}}{2} \times \text{area}/[\pi(\text{length}/2)]. \qquad (1)$$

The volumes at end systole (VolS) and end diastole (VolD) were measured and used to calculate stroke volume (SV = VolD − VolS) and ejection fraction (EF% = endocardial SV/endocardial VolD × 100). Cardiac output (CO = SV × heart rate) was calculated from stroke volume and heart rate. Mitral valve E and A wave inflow velocities were sampled at the tips of the leaflets of the mitral valve from the apical 4-chamber view. Doppler tissue imaging was performed with acquisition of peak E′ velocity from the lateral (E′la) and septal annulus (E′sa) of the mitral valve imaged from the apical 4-chamber view. Isovolumic relaxation time, from the closure of the aortic valve to the opening of the mitral valve, was measured from the apical 5-chamber view using Doppler flow imaging. Imaging was performed at 8 hours after CLP.

Mitochondrial mass and membrane potential ψYm

The cell-permeable carbocyanine-based MitoTracker Deep Red (Invitrogen) was used to measure mitochondrial mass in CMs and other features. This dye is cell permeable, accumulating selectively in mitochondria. Flow cytometry was performed as described above. The mitochondrial membrane potential was obtained by using the dye, tetramethylrhodamine, ethyl ester (TMRE; Mitochondrial Membrane Potential Assay Kit; Abcam, Cambridge, MA, USA). TMRE is cell-permeable, positively charged, and accumulates in active mitochondria because of the relative negative charge of mitochondria. Carbonyl cyanide 4-(trifluoromethoxy)phenylhydrazone (FCCP) is an ionophore uncoupler of oxidative phosphorylation, which eliminates mitochondrial membrane potential and TMRE staining and is used as a control.

ATP detection in CMs

Total levels of cellular ATP were obtained by using the Luminescent ATP Detection Assay Kit (Abcam, Cambridge, MA, USA). In brief, the kit is based on firefly (*Photinus pyralis*) luciferase and determines the total level of cellular ATP. The cells were plated with 12,000 cells per well in a 96-well plate. The kit is based on the production of light caused by reaction of ATP with added luciferase and D-luciferin, using Infinite F200 luminescence instrument (Tecan, Salsburg, Austria).

FITC-labeled histones

FITC (37.5 μg; Sigma-Aldrich) was conjugated to 1 mg mixed calf thymus histones. For *in vivo* experiments 45 mg/kg body weight histones were injected intravenously, and FITC in heart homogenates was analyzed by fluorescence plate reader (excitation, 485 nm; emission, 535 nm).

Confocal imaging

For confocal imaging, CMs were cultured on sterile glass coverslips coated with natural mouse Laminin (Life Technologies). Cells were incubated with FITC-conjugated histones for 30 minutes and then washed and fixed. Confocal imaging was performed with a Zeiss LSM 510 Confocal microscope (Zeiss USA, Pleasanton, CA, USA).

Statistical analysis

All values were expressed as means ± SEM. Datasets were analyzed by 1-way ANOVA followed by Dunnett's or Tukey's multiple comparison test or by Student *t* test. $P < 0.05$ was considered statistically significant. GraphPad Prism 6.0 software was used for statistical analysis (GraphPad Software, Incorporated, San Diego, CA, USA). In the case of echocardiogram/Doppler data, each mouse was tested before and 8 hours after CLP, allowing paired *t* testing analysis for each mouse.

RESULTS

Requirements for appearance of plasma histones after CLP

These studies were designed to measure appearance in plasma of extracellular histones after CLP, the extent to which both C5a receptors were required for histone presence, the requirement for PMNs, evidence for the role of the NLRP3 inflammasome, and evidence that intravenously infusion of FITC-labeled histones resulted in buildup in CMs. C57BL/6 young adult (20–30 g) male mice underwent CLP as described earlier (19). The data in **Fig. 1A** indicate that plasma histones were detected (by ELISA technology) 6 hours after CLP in wild-type (WT) mice and persisted for 24 hours, followed by reduction. Fig. 1*B* indicates that the absence of either C5a receptor (C5aR1 and C5aR2) resulted in a nearly 80% fall in plasma histone levels after CLP, whereas PMN depletion caused a 77% reduction in plasma levels of histones 12 h after CLP (Fig. 1*C*), indicating a linkage between histone appearance after CLP and PMN availability and C5a receptors. Fig. 1*D* shows a requirement for the NLRP3 protein inflammasome in histone buildup in plasma after CLP, because absence of NLRP3 protein or caspase 1 resulted in 69% and 84% reductions, respectively, in plasma histone levels 16 h after CLP. The data in Fig. 1*E* indicate that FITC-labeled histones given intravenously to WT (non-CLP) mice localized in the heart 30 minutes later. In Fig. 1*F*, when CMs were exposed *in vitro* to FITC histones, histone localization could be seen both on
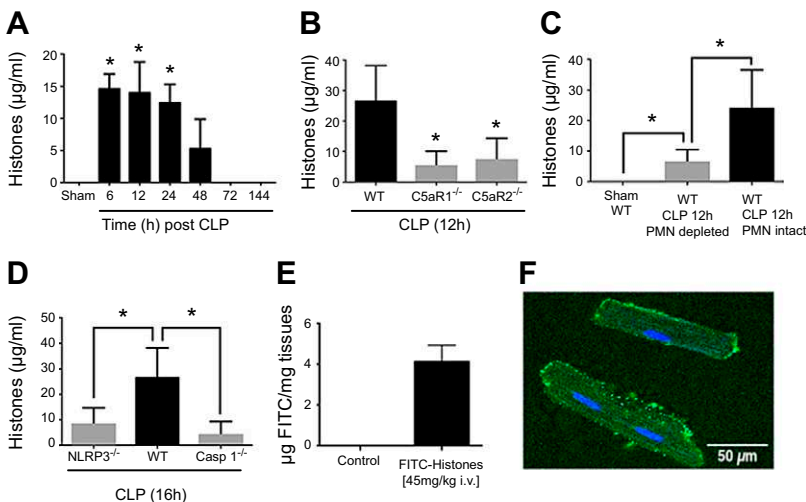

Figure 1. Requirements for histone appearance in plasma after CLP and binding of histones to CMs. *A*) Time course (hours) for extracellular histone appearance in plasma from C57BL/6 (WT) mice after CLP. *B*) Requirements for both C5a receptors (C5aR1, C5aR2) for histone appearance in plasma 12 hours after CLP. *C*) PMN dependence for histone appearance in plasma 12 h after CLP, using the mAb that depletes blood PMN *via* reactivity with the Ly-6G epitope on PMNs. *D*) Histone appearance in plasma after CLP is dependent on the NLRP3 inflammasome. *E*) Thirty min after intravenous infusion of FITC-histones (45 mg/kg body weight) into WT mice, heart homogenates contained histones. *F*) Confocal microscopy of rat CMs exposed *in vitro* to fluorescein-labeled histones (50 μg/ml) for 30 minutes at 37°C, showing both surface binding of histones (upper), as well as evidence of histone internalization into CM cytosol (lower). Nuclei are defined by DAPI stain (blue). For all frames, $n \geq 6$ for each bar. *Differences were significant, $P < 0.05$ (*A*) *vs.* sham and (*B*) *vs.* WT, or as indicated.

the plasma membrane (upper CM) and in the cytosol (lower CM) of cells.

Increased ROS and $[Ca^{2+}]_i$ in CMs exposed to histones

Because there is published evidence that CLP perturbs the redox status and may feature buildup of $[Ca^{2+}]_i$ in CMs, a series of *in vitro* and *in vivo* studies involving changes in CMs exposed to histones was carried out. We assessed the ability of histones to cause elevations in ROS and $[Ca^{2+}]_i$ in mouse CMs, using flow cytometric techniques. CMs were loaded with fluro-3 AM or with Cell ROX Deep Red. In **Fig. 2A**, a histone mixture in a dose-dependent manner (0.5–100 μg/ml) caused increased cytosolic ROS in CMs and related to the duration of exposure of CMs (10–60 min; Fig. 2B). In Fig. 2C, when histones were infused intravenously (65 mg/kg body weight) into WT mice, CMs isolated 30 minutes later showed a significant increase in cytosolic ROS as detected by flow cytometry compared with sham CMs (control). In Fig. 2D–G, increases in CM $[Ca^{2+}]_i$ after histone exposure *in vitro* were time dependent (Fig. 2D) and dose dependent (Fig. 2E). Intravenous infusion of the histone mixture increased $[Ca^{2+}]_i$ in mouse CMs (Fig. 2F), as was the case with cytosolic ROS. After *in vitro* exposure to histone concentrations in the range found in plasma after CLP (Fig. 1A), $[Ca^{2+}]_i$ increases were magnified in CMs from CLP mice compared with non-CLP CMs (Fig. 2G). When WT and TLR-null ($TLR2^{-/-}$ or $TLR4^{-/-}$) mice were infused intravenously with histones, 30 minutes later $[Ca^{2+}]_i$ was increased in CMs from WT mice (Fig. 2H, black bar *vs.* white bar), but not in CMs from $TLR2^{-/-}$ or $TLR4^{-/-}$ mice (gray bars), consistent with the literature suggesting that histones function as ligands for these TLRs (7–9).
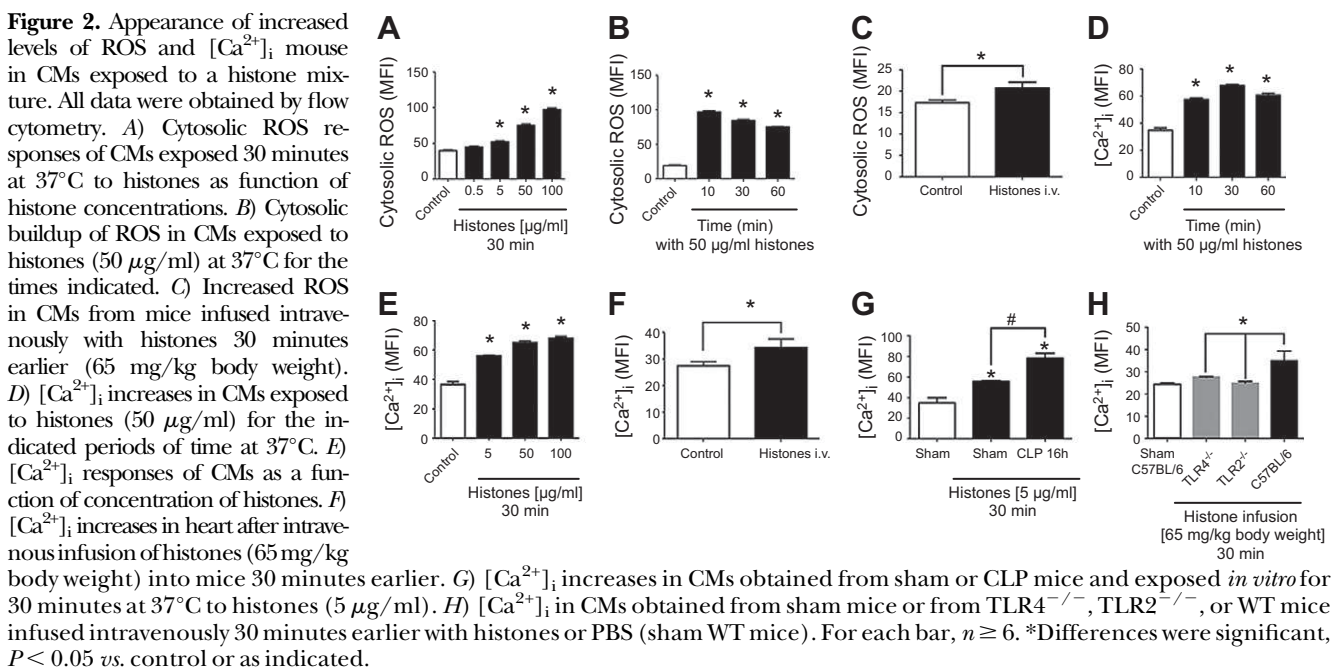
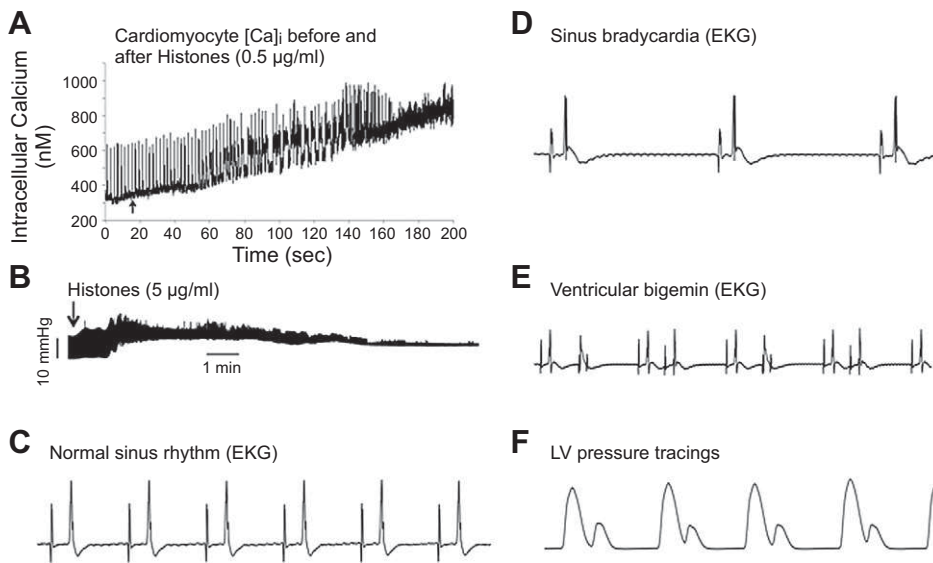## Functional defects in CMs and hearts after exposure to histones

We assessed effects of histones on single isolated mouse CMs preloaded with Fluo3 AM and electrically paced as

described elsewhere (22). Details are provided in the Materials and Methods. In addition, mouse hearts perfused with histones were assessed for changes in left ventricle (LV) pressures and ECG tracings. Details of Langendorff perfusion techniques are described elsewhere (20, 21). As shown in **Fig. 3A**, there were progressive increases in baseline $[Ca^{2+}]_i$ after addition of histones to electrically paced CMs, indicating defective $[Ca^{2+}]_i$ clearance during diastole, as well as a widening of the Ca^{2+} transients and a progressively rising baseline for $[Ca^{2+}]_i$. There was a progressive reduction in the amplitudes of the calcium transients. In **Fig. 4**, the tracings were magnified to emphasize widening of the calcium transients after CM exposure to histones. Less than 1 minute after addition of histones, Ca^{2+} transients began to widen (Fig. 4, lower), indicating defective cytosolic clearance of Ca^{2+} in CMs. In Fig. 3B, Langendorff mouse hearts (WT) perfused with the histone mixture showed progressive reductions and narrowing of LV pressure tracings, indicating defects in contractility responses. In Fig. 3C–E, ECG tracings demonstrated normal sinus rhythm (Fig. 3C) and histone-induced arrhythmias: sinus bradycardia (Fig. 3D) and ventricular bigeminy (Fig. 3E). Bigeminy was confirmed by LV pressure recordings (Fig. 3F). Accordingly, histones *in vitro* induced a variety of defects that would be expected to have important negative functional consequences on heart performance.

Histone-induced defects in mitochondria

Functional mitochondria are essential for cardiac functions. **Fig. 5** shows histone effects on mitochondria in rat CMs, in some cases using compounds that are cell permeable and mitochondrial seeking. Rat CMs were used because of their abundance and stability as contrasted to mouse CMs. In Fig. 5A, high concentrations of histones (≥ 500 μg/ml) caused annexin V binding to CMs, a feature predictive of apoptosis. In Fig. 5B, we used a mitochondrial membrane potential indicator dye (TMRE), which is cell permeable, its charge (positive) resulting in a buildup in

Figure 2. Appearance of increased levels of ROS and $[Ca^{2+}]_i$ mouse in CMs exposed to a histone mixture. All data were obtained by flow cytometry. *A)* Cytosolic ROS responses of CMs exposed 30 minutes at 37°C to histones as function of histone concentrations. *B)* Cytosolic buildup of ROS in CMs exposed to histones (50 μg/ml) at 37°C for the times indicated. *C)* Increased ROS in CMs from mice infused intravenously with histones 30 minutes earlier (65 mg/kg body weight). *D)* $[Ca^{2+}]_i$ increases in CMs exposed to histones (50 μg/ml) for the indicated periods of time at 37°C. *E)* $[Ca^{2+}]_i$ responses of CMs as a function of concentration of histones. *F)* $[Ca^{2+}]_i$ increases in heart after intravenous infusion of histones (65 mg/kg

body weight) into mice 30 minutes earlier. *G)* $[Ca^{2+}]_i$ increases in CMs obtained from sham or CLP mice and exposed *in vitro* for 30 minutes at 37°C to histones (5 μg/ml). *H)* $[Ca^{2+}]_i$ in CMs obtained from sham mice or from $TLR4^{-/-}$, $TLR2^{-/-}$, or WT mice infused intravenously 30 minutes earlier with histones or PBS (sham WT mice). For each bar, $n \geq 6$. *Differences were significant, $P < 0.05$ *vs.* control or as indicated.

Figure 3. Histones cause increases in $[Ca^{2+}]_i$ in CMs and physiologic defects in perfused hearts. Ability of histones to cause defects in paced CMs before or after histone addition (at time 0) (*A*) or in Langendorff mouse hearts perfused with histones (at arrows) (*B–F*). LV pressures were measured (*B, F*) and also monitored by ECG tracings (*C–E*). *A*) Isolated cardiomyocytes were loaded with an intracellular calcium indicator (Fluo3 AM) and calcium change was measured during electrical pacing (0.5 Hz). Histones caused calcium overload in cardiomyocytes. *B*) LV pressures in Langendorff mouse hearts showing falling and narrowing of pressure tracings after perfusion with histones (arrow). *C–E*) ECG tracings of perfused mouse hearts before (normal sinus rhythm) (*C*) and after histone exposure, which caused sinus bradycardia (*D*) and ventricular bigeminy (*E*), which was confirmed by LV pressure tracings (*F*). Tracings are representative of 11 independent experiments.

active mitochondria (which bear a negative charge). FCCP is an ionophore that uncouples oxidative phosphorylation, eliminating the mitochondrial membrane potential and TMRE staining, which were used as controls. There was a progressive loss of mitochondrial membrane potential caused by exposure of CMs to increasing concentrations of histones. CMs exposed to histones also had dramatic

Figure 4. Expanded tracings of $[Ca^{2+}]_i$ in CMs before and after histone addition. Expanded intracellular calcium tracings (from Fig. 3) in electrically paced CMs (0.5 mHz) before (*A*) and after (*B*) addition of the histone mixture (5 µg/ml). In the lower panel, there was expanding width of intracellular calcium tracings, indicating defective $[Ca^{2+}]_i$ clearance during diastole. Tracings are representative of patterns in which $n \geq 4$ each.

reductions in ATP as a function of histone concentrations (Fig. 5*C*). Levels of ATP were obtained using a luminescent ATP detection assay kit. Finally, histones caused dose-dependent increases in mitochondrial mass as assessed by flow cytometry (Fig. 5*D*), likely because of the buildup of fluids within mitochondria (resulting in swelling). Interestingly, several of these responses occurred within the dose range of histones appearing in plasma after CLP (Fig. 1*A*).
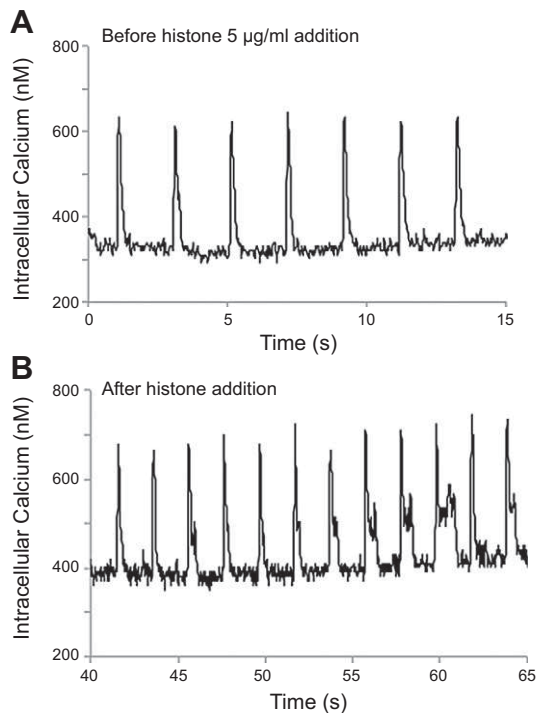
Direct evidence for the role of histones in cardiac dysfunctions after sepsis

To determine whether a linkage exists between histones and the *in vivo* functional defects in cardiovascular performance developing after CLP (**Fig. 6**), ECHO/Doppler parameters were measured before (white bars) and 8 h after CLP (black and gray bars). In CLP mice, 65 µg isotype-matched IgG isolated from normal serum from mice (nsIgG) (gray bars) or with 65 µg neutralizing mAb to histones (black bars) were infused intravenously just before CLP. Mice subjected to CLP demonstrated significant abnormalities in systolic (Fig. 6*A–D*) and diastolic (Fig. 6*E–H*) parameters that were partially or completely reversed by administration of neutralizing mAb to histones. For instance, CLP mice given nsIgG (gray bars) demonstrated modest but significantly decreased heart rates, whereas mice treated with a neutralizing mAb to histones had heart rates similar to sham-operated controls (Fig. 6*A*, white *vs.* black and gray bars). CLP also caused a substantial decrease in LV stroke volume (black bar) and cardiac output (Fig. 6*B, C*) (white *vs.* gray bars). mAb treatment partially reversed the decrement in stroke volume (Fig. 6*B*), whereas the cardiac output in CLP mice given the histone-neutralizing mAb was comparable to sham-operated controls (Fig. 6*B*). The CLP-mediated decrease in cardiac output did not appear to be caused by direct myocardial depression, because the LV ejection fraction was increased after CLP and further increased by histone

Figure 5. Changes in CMs and CM mitochondria exposed (37°C, 30 minutes) to increasing concentrations of histones. *A*) Binding of annexin V to CMs after exposure to a range of concentrations of the histone mixture. *B*) Reductions in mitochondrial membrane potential after exposure to increasing concentrations of the histone mixture. *C*) Reductions in mitochondrial ATP levels after increasing concentrations of histones (37°C for 60 minutes). *D*) Increases in mitochondrial mass following exposure to increasing concentrations of the histone mixture (37°C for 60 minutes). For each bar, $n \geq 4$. *Differences were significant, $P < 0.05$ *vs.* control.
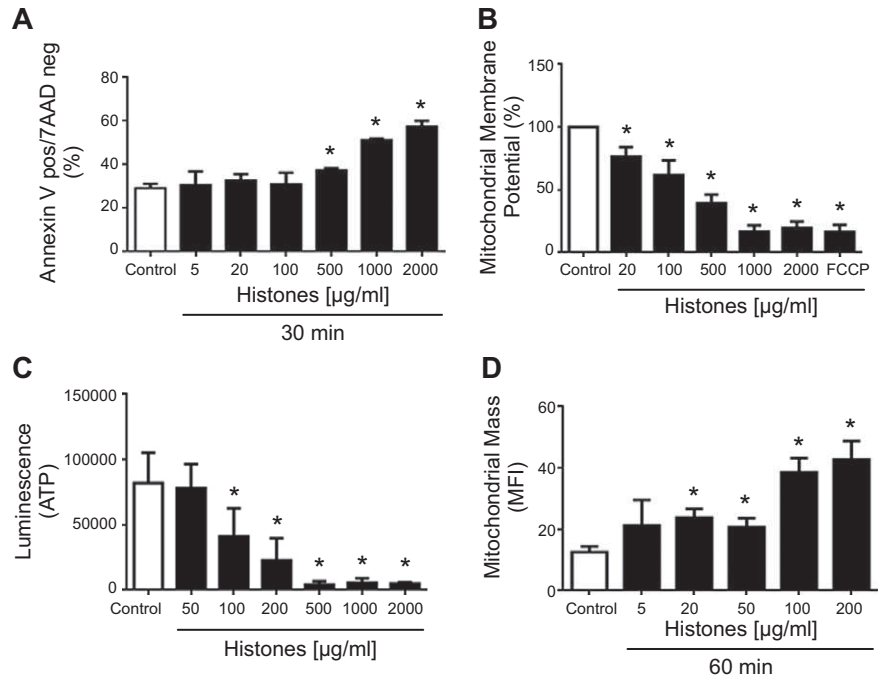
mAb infusion (Fig. 6*D*). Therefore, reduced cardiac output 8 h after CLP was primarily caused by changes in ventricular volumes and heart rates rather than direct myocardial suppression.

The diastolic abnormalities caused by CLP were also prevented by histone mAb infusion (Fig. 6*E*–*H*). Isovolumic relaxation was significantly prolonged 8 hours after CLP but was restored to normal by histone mAb treatment (Fig. 6*E*). Doppler tissue imaging revealed decreased passive filling (E′) velocities at the septal (Fig. 6*F*) and lateral (Fig. 6*G*) mitral valve annulus 8 h after CLP.

Infusion of mAb prevented the abnormalities in mitral annular velocities after CLP. The decreased end diastolic volume noted after CLP was not significantly improved by histone mAb infusion (Fig. 6*H*). This suggests that changes in ventricular volumes after CLP may be caused by third space fluid losses affecting loading conditions. In contrast, the cardiac diastolic dysfunction observed after CLP may be caused by elevations in $[Ca^{2+}]_i$ in CMs in response to histone exposure. These abnormalities were prevented by infusion of mAb to histones (black *vs.* white bars), whereas nonspecific IgG (gray bars) was not protective.
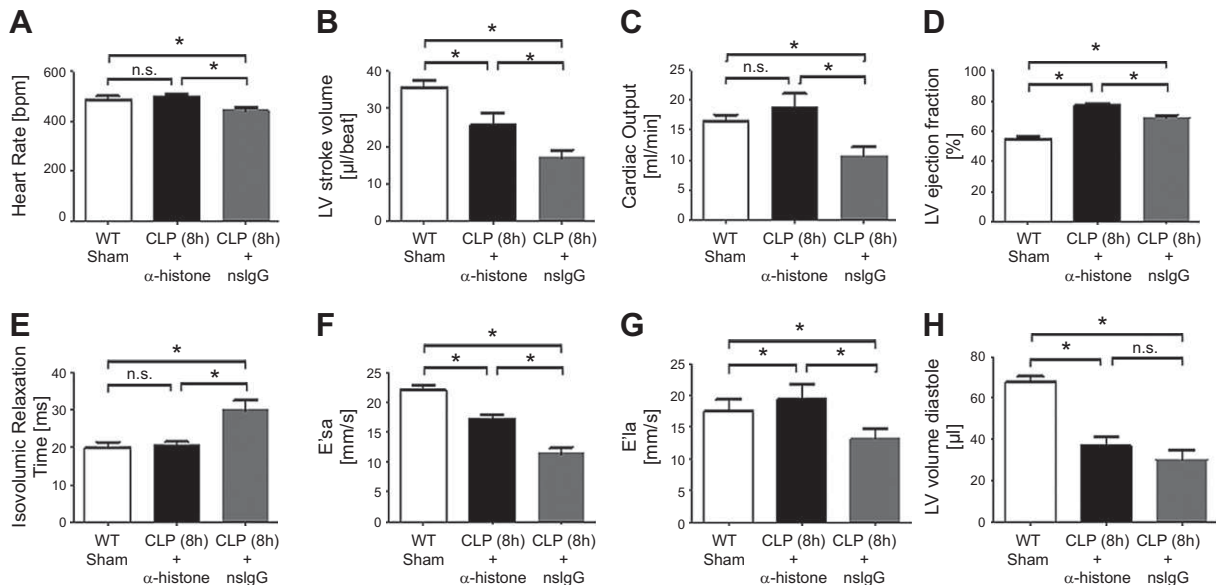

Figure 6. *In vivo* induction of cardiac dysfunction by histones after CLP. Heart functional parameters in normal WT mice (WT sham, white bars), CLP mice receiving isotype-matched IgGκ (nsIgG, gray bars), or mAb with neutralizing activity to H2A and H4 (α-histone, black bars) (13); 65 μg of antibody was given i.v. at time 0, and ECHO/Doppler parameters were measured before and 8 h after CLP in each mouse. *A*) Heart rates. *B*) Left ventricular stroke volume after CLP. *C*) Cardiac output. *D*) LV ejection fraction. *E*) Isovolumic relaxation. *F*–*H*) Doppler tissue imaging parameters of mitral valve function. *H*) LV volume diastole. For each bar, $n \geq 6$ mice. *Differences between groups were significant as indicated, $P < 0.05$.

DISCUSSION

The linkage between histone appearance and cardiac dysfunction during sepsis is described in this report. It is known that infusion of large amounts of histones into mice results in multiorgan failure and death (10). In heart failure (24) or during myocardial remodeling after ischemia-reperfusion injury (25), histones may play a role in cardiac dysfunction, although the evidence is limited. After intravenous injection of histones into mice, pulmonary hypertension and right-sided heart failure developed and were followed by ventricular arrest, associated with histone-induced thromboembolism in the lungs. Platelet-depleted mice were transiently protected from histone-mediated death within the first 30 min, but the protective effects of platelet depletion disappeared soon thereafter (26), suggesting that additional cellular and molecular mechanisms are involved in histone-induced cardiac dysfunction during sepsis.

In the data presented in this report, we confirmed the appearance of histones in plasma after CLP, similar to an earlier report (9), and provided evidence that use of an mAb that has neutralizing activities to histones (H2A, H4) (17) reduces or abolishes defects in systolic and diastolic function in the heart appearing after CLP, based on ECHO/Doppler parameters. These findings are consistent with observations that neutralizing antibodies against histones reduced mortality in mice infused with TNF or LPS, as well as in mice with sepsis following CLP (10).

In an ex vivo model, Langendorff-perfused mouse hearts showed progressive reductions in LV pressure tracings after perfusion with histones, resulting in defects in contractility responses (Fig. 3). Studies in septic humans using echocardiography demonstrated slower left ventricular filling and aberrant left ventricular relaxation time (27, 28), suggesting that impaired compliance may contribute to myocardial depression during sepsis. The current studies establish a direct relationship between histones and cardiac dysfunction in sepsis following CLP.

The requirement of PMNs for histone appearance in plasma after CLP in our current study is similar to our recent report in ALI in which PMN depletion reduced the histone appearance in BALF (14). As well, histones were found in BALFs from humans with ALI. Our recent report also describes the requirement for the NLRP3 inflammasome in developing ALI and demonstrates that *in vitro* activation of PMNs by C5a can cause the appearance of histones in supernatant fluids, presumably released from neutrophil extracellular traps (NETs) (29). Histones in plasma obtained from mice 8 hours after CLP were significantly reduced in the absence of C5aR1, C5aR2, or NLRP3, linking the complement and innate immune systems. Observations describing improved survival in CLP mice with genetic deficiency of either C5aR1 or C5aR2 (30) denote a linkage between C5a, its receptors, and histone release in sepsis. Furthermore, histones promoted thrombus formation (31) and were found to enhance plasma thrombin generation (32). **Fig. 7** describes the pathways in sepsis leading to histones appearance and ultimate cardiac dysfunction. Accordingly, thrombin is also known to generate C5a from C5 (in the absence of C3), the product being biologically active and structurally identical to C5a generated by the C5 convertase (33). Thrombin
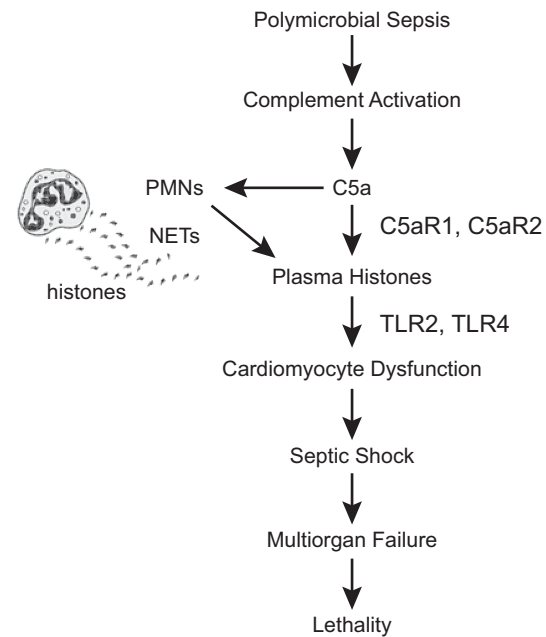

Figure 7. The cardiomyopathy of sepsis requires C5a, its receptors, and PMNs, whereas cardiac dysfunction is linked to appearance of histones. Proposed sequence of events after CLP (polymicrobial sepsis), leading to complement activation, with dependence on C5a receptors and PMNs for histone appearance in plasma. Histones, which interact with TLR2 and TLR4 on a variety of cell types, including CMs, cause cell damage, organ dysfunction, and lethality.

potentially can act as an amplifier of complement effector generation. Another activator of C5 found in trauma patients is factor VII-activating protease, which is activated by histones (34). In summary, the data in this report indicate that the appearance of extracellular histones in plasma after CLP engages 3 arms of the innate immune system: the complement system (C5a and its receptors), PMNs, and the NLRP3 inflammasome. Although the precise links that orchestrate these connections are inadequately understood, it seems likely that the early initiating events in sepsis are complement activation with C5a generation and engagement of both C5aR1 and C5aR2 (Fig. 7).

The mechanism of histone-induced cell injury is unclear. Calcium influx caused by plasma membrane disruption (12) may be a mechanism of histone-induced toxicity. In our studies, histones cause impressive elevations in $[Ca^{2+}]_i$ in CMs, as measured by flow cytometry. Electrophysiological measurements in paced cardiomyocytes exposed to histones confirmed an accumulation of cytosolic calcium (Fig. 3). In CMs, this buildup was independent of translocation of extracellular Ca^{2+} into the CMs (data not shown). Defective Ca^{2+} handling in the cytosol caused by reduced Ca^{2+} sequestration into the sarcoplasmic reticulum has been found in the failing human myocardium (35). These findings are contrary to studies showing in endothelial cells that calcium influx from extracellular sites is associated with histone-induced damage (12) and that cell dysfunction caused by histones may be related to the interaction of histones with membrane

phospholipid bilayers (36), followed by an increase of membrane permeability (37). In our studies, isolated CMs incubated with histones *in vitro* showed accumulation of histones on the cell membrane and in the cytosol (Fig. 1*F*). There are suggestions that *in vitro* and *in vivo* responses to DAMPs require TLR2 and TLR4 (9, 10, 38). When wild-type and TLR-null (TLR2$^{-/-}$ or TLR4$^{-/-}$) mice were infused intravenous with histones, 30 minutes later [Ca^{2+}]$_i$ was increased in CMs from WT, but not in CMs from TLR2$^{-/-}$ or TLR4$^{-/-}$, mice (Fig. 2*H*). Such data are consistent with reports suggesting that histones may function as ligands for TLR2 and TLR4 (8, 9). Interestingly, TLR2 and 4 were found to be involved in plasma prothrombin activation (32), which resulted in amplified C5a generation.

CMs isolated after infusion of extracellular histones showed, as did cultured CMs in the presence of histones, increases in cytosolic and nuclear/mitochondrial ROS (Fig. 2). ROS may play an important role in the pathogenesis of myocardial dysfunction in cardiovascular diseases, such as ventricular hypertrophy, heart failure, atrial fibrillation, and myocardial ischemia (39). Redox sensitive signaling pathways are critically involved in multiple CM functions such as contractile performance, rhythmicity, hypertrophy, and responses to stress (40). ROS modulates Ca^{2+} handling proteins by oxidation of thiol (-SH) groups, leading to Ca^{2+} increases of the cytosol (41), as well as blocking ATP-binding sites on SERCA2, resulting in cytosolic Ca^{2+} overload (42). Collectively, our data suggest that histones induce elevations in CM ROS and [Ca^{2+}]$_i$ that may be linked to defective CM function, as also suggested in other reports (39, 40, 43, 44).

The combination of histones, together with oxidants and proteases from both PMNs and macrophages, seems to represent the distal pathways leading to organ injury, as summarized in Fig. 7. In the present studies, we showed that treatment of isolated CMs with histones resulted in decreased mitochondrial membrane potential and decreased ATP levels, which have been associated with cardiac dysfunction (45–47). Interestingly, these intracellular changes occurred within the dose ranges of histones appearing in plasma after CLP. In our studies, we found increased annexin V binding in cardiomyocytes exposed to high concentrations of histones. Our data indicate that in polymicrobial sepsis, complement activation lends to C5a generation and its engagement with C5aR1 and C5aR2, collectively resulting in NET formation and release of histones. Histones presumably function as ligands for TLR2 and 4, associated with cardiac dysfunction, septic shock, and lethality. Increased intracellular calcium and cytochrome c released from damaged mitochondria (48, 49) may amplify apoptotic signals. It is important to note that induction of apoptosis in CMs required doses of histones that were beyond plasma levels of histones in CLP mice (Fig. 1). Such observations would be consistent with recent reports in which autopsy from patients with severe sepsis or septic shock failed to reveal evidence of myocardial apoptosis (50), as well as with reports that cardiac MRI analysis performed 6 weeks after early imaging in sepsis showed complete recovery of cardiac contractility (51). Finally, the importance of C5a and its receptors in histone production in sepsis is underscored by a recent review that emphasizes how the complement and coagulation systems collaborate to generate C5a in a variety of situations in which inflammatory injury occurs (52).

Taken together, our results suggest that the presence of extracellular histones occurring after CLP can be linked to appearance of defects in cardiac function during sepsis. Neutralizing histone antibodies or drugs that block histone interactions with CMs may be potential therapeutic strategies to prevent or ameliorate septic cardiomyopathy. It is also possible that histone neutralization combined with a neutralizing mAb to C5a might represent an effective strategy for treatment of patients with sepsis. [Fj]

REFERENCES

1. Charpentier, J., Luyt, C. E., Fulla, Y., Vinsonneau, C., Cariou, A., Grabar, S., Dhainaut, J. F., Mira, J. P., and Chiche, J. D. (2004) Brain natriuretic peptide: A marker of myocardial dysfunction and prognosis during severe sepsis. *Crit. Care Med.* **32**, 660–665

2. Celes, M. R., Prado, C. M., and Rossi, M. A. (2013) Sepsis: going to the heart of the matter. *Pathobiology* **80**, 70–86

3. Rudiger, A., and Singer, M. (2007) Mechanisms of sepsis-induced cardiac dysfunction. *Crit. Care Med.* **35**, 1599–1608

4. Parker, M. M., Shelhamer, J. H., Bacharach, S. L., Green, M. V., Natanson, C., Frederick, T. M., Damske, B. A., and Parrillo, J. E. (1984) Profound but reversible myocardial depression in patients with septic shock. *Ann. Intern. Med.* **100**, 483–490

5. Seong, S. Y., and Matzinger, P. (2004) Hydrophobicity: an ancient damage-associated molecular pattern that initiates innate immune responses. *Nat. Rev. Immunol.* **4**, 469–478

6. Denk, S., Perl, M., and Huber-Lang, M. (2012) Damage- and pathogen-associated molecular patterns and alarmins: keys to sepsis? *Eur. Surg. Res.* **48**, 171–179

7. Boyd, J. H., Mathur, S., Wang, Y., Bateman, R. M., and Walley, K. R. (2006) Toll-like receptor stimulation in cardiomyocytes decreases contractility and initiates an NF-kappaB dependent inflammatory response. *Cardiovasc. Res.* **72**, 384–393

8. Allam, R., Scherbaum, C. R., Darisipudi, M. N., Mulay, S. R., Hägele, H., Lichtnekert, J., Hagemann, J. H., Rupanagudi, K. V., Ryu, M., Schwarzenberger, C., Hohenstein, B., Hugo, C., Uhl, B., Reichel, C. A., Krombach, F., Monestier, M., Liapis, H., Moreth, K., Schaefer, L., and Anders, H. J. (2012) Histones from dying renal cells aggravate kidney injury via TLR2 and TLR4. *J. Am. Soc. Nephrol.* **23**, 1375–1388

9. Xu, J., Zhang, X., Monestier, M., Esmon, N. L., and Esmon, C. T. (2011) Extracellular histones are mediators of death through TLR2 and TLR4 in mouse fatal liver injury. *J. Immunol.* **187**, 2626–2631

10. Xu, J., Zhang, X., Pelayo, R., Monestier, M., Ammollo, C. T., Semeraro, F., Taylor, F. B., Esmon, N. L., Lupu, F., and Esmon, C. T. (2009) Extracellular histones are major mediators of death in sepsis. *Nat. Med.* **15**, 1318–1321

11. Ostrowski, S. R., Berg, R. M., Windeløv, N. A., Meyer, M. A., Plovsing, R. R., Møller, K., and Johansson, P. I. (2013) Coagulopathy, catecholamines, and biomarkers of endothelial damage in experimental human endotoxemia and in patients with severe sepsis: a prospective study. *J. Crit. Care* **28**, 586–596

12. Abrams, S. T., Zhang, N., Manson, J., Liu, T., Dart, C., Baluwa, F., Wang, S. S., Brohi, K., Kipar, A., Yu, W., Wang, G., and Toh, C. H. (2013) Circulating histones are mediators of trauma-associated lung injury. *Am. J. Respir. Crit. Care Med.* **187**, 160–169

13. Kutcher, M. E., Xu, J., Vilardi, R. F., Ho, C., Esmon, C. T., and Cohen, M. J. (2012) Extracellular histone release in response to traumatic injury: implications for a compensatory role of activated protein C. *J. Trauma Acute Care Surg.* **73**, 1389–1394

14. Bosmann, M., Grailer, J. J., Ruemmler, R., Russkamp, N. F., Zetoune, F. S., Sarma, J. V., Standiford, T. J., and Ward, P. A. (2013) Extracellular histones are essential effectors of C5aR- and C5L2-mediated tissue damage and inflammation in acute lung injury. *FASEB J.* **27**, 5010–5021

15. Gerard, N. P., Lu, B., Liu, P., Craig, S., Fujiwara, Y., Okinaga, S., and Gerard, C. (2005) An anti-inflammatory function for the complement anaphylatoxin C5a-binding protein, C5L2. *J. Biol. Chem.* **280**, 39677–39680

16. Höpken, U. E., Lu, B., Gerard, N. P., and Gerard, C. (1996) The C5a chemoattractant receptor mediates mucosal defence to infection. *Nature* **383**, 86–89

17. Monestier, M., Fasy, T. M., Losman, M. J., Novick, K. E., and Muller, S. (1993) Structure and binding properties of monoclonal antibodies to core histones from autoimmune mice. *Mol. Immunol.* **30**, 1069–1075

18. Baker, C. C., Chaudry, I. H., Gaines, H. O., and Baue, A. E. (1983) Evaluation of factors affecting mortality rate after sepsis in a murine cecal ligation and puncture model. *Surgery* **94**, 331–335

19. Rittirsch, D., Huber-Lang, M. S., Flierl, M. A., and Ward, P. A. (2009) Immunodesign of experimental sepsis by cecal ligation and puncture. *Nat. Protoc.* **4**, 31–36

20. Kaestner, L., Scholz, A., Hammer, K., Vecerdea, A., Ruppenthal, S., and Lipp, P. (2009) Isolation and genetic manipulation of adult cardiac myocytes for confocal imaging. *J. Vis. Exp.* (31)

21. Louch, W. E., Sheehan, K. A., and Wolska, B. M. (2011) Methods in cardiomyocyte isolation, culture, and gene transfer. *J. Mol. Cell. Cardiol.* **51**, 288–298

22. Herron, T. J., Vandenboom, R., Fomicheva, E., Mundada, L., Edwards, T., and Metzger, J. M. (2007) Calcium-independent negative inotropy by beta-myosin heavy chain gene transfer in cardiac myocytes. *Circ. Res.* **100**, 1182–1190

23. Boluyt, M. O., Converso, K., Hwang, H. S., Mikkor, A., and Russell, M. W. (2004) Echocardiographic assessment of age-associated changes in systolic and diastolic function of the female F344 rat heart. *J. Appl. Physiol.* **96**, 822–828

24. Yamamichi, S., Fujiwara, Y., Kikuchi, T., Nishitani, M., Matsushita, Y., and Hasumi, K. (2011) Extracellular histone induces plasma hyaluronan-binding protein (factor VII activating protease) activation *in vivo*. *Biochem. Biophys. Res. Commun.* **409**, 483–488

25. Tingare, A., Thienpont, B., and Roderick, H. L. (2013) Epigenetics in the heart: the role of histone modifications in cardiac remodelling. *Biochem. Soc. Trans.* **41**, 789–796

26. Nakahara, M., Ito, T., Kawahara, K., Yamamoto, M., Nagasato, T., Shrestha, B., Yamada, S., Miyauchi, T., Higuchi, K., Takenaka, T., Yasuda, T., Matsunaga, A., Kakihana, Y., Hashiguchi, T., Kanmura, Y., and Maruyama, I. (2013) Recombinant thrombomodulin protects mice against histone-induced lethal thromboembolism. *PLoS ONE* **8**, e75961

27. Munt, B., Jue, J., Gin, K., Fenwick, J., and Tweeddale, M. (1998) Diastolic filling in human severe sepsis: an echocardiographic study. *Crit. Care Med.* **26**, 1829–1833

28. Jafri, S. M., Lavine, S., Field, B. E., Bahorozian, M. T., and Carlson, R. W. (1990) Left ventricular diastolic function in sepsis. *Crit. Care Med.* **18**, 709–714

29. Grailer, J. J., Canning, B. A., Kalbitz, M., Haggadone, M. D., Dhond, R. M., Andjelkovic, A. V., Zetoune, F. S., and Ward, P. A. (2014) Critical role for the NLRP3 inflammasome during acute lung injury. *J. Immunol.* **192**, 5974–5983

30. Rittirsch, D., Flierl, M. A., Nadeau, B. A., Day, D. E., Huber-Lang, M., Mackay, C. R., Zetoune, F. S., Gerard, N. P., Cianflone, K., Köhl, J., Gerard, C., Sarma, J. V., and Ward, P. A. (2008) Functional roles for C5a receptors in sepsis. *Nat. Med.* **14**, 551–557

31. Fuchs, T. A., Brill, A., Duerschmied, D., Schatzberg, D., Monestier, M., Myers, D. D., Jr., Wrobleski, S. K., Wakefield, T. W., Hartwig, J. H., and Wagner, D. D. (2010) Extracellular DNA traps promote thrombosis. *Proc. Natl. Acad. Sci. USA* **107**, 15880–15885

32. Semeraro, F., Ammollo, C. T., Morrissey, J. H., Dale, G. L., Friese, P., Esmon, N. L., and Esmon, C. T. (2011) Extracellular histones promote thrombin generation through platelet-dependent mechanisms: involvement of platelet TLR2 and TLR4. *Blood* **118**, 1952–1961

33. Huber-Lang, M., Sarma, J. V., Zetoune, F. S., Rittirsch, D., Neff, T. A., McGuire, S. R., Lambris, J. D., Warner, R. L., Flierl, M. A., Hoesel, L. M., Gebhard, F., Younger, J. G., Drouin, S. M., Wetsel, R. A., and Ward, P. A. (2006) Generation of C5a in the absence of C3: a new complement activation pathway. *Nat. Med.* **12**, 682–687

34. Kanse, S. M., Gallenmueller, A., Zeerleder, S., Stephan, F., Rannou, O., Denk, S., Etscheid, M., Lochnit, G., Krueger, M., and Huber-Lang, M. (2012) Factor VII-activating protease is activated in multiple trauma patients and generates anaphylatoxin C5a. *J. Immunol.* **188**, 2858–2865

35. Pieske, B., Maier, L. S., Bers, D. M., and Hasenfuss, G. (1999) Ca2+ handling and sarcoplasmic reticulum Ca2+ content in isolated failing and nonfailing human myocardium. *Circ. Res.* **85**, 38–46

36. Kleine, T. J., Lewis, P. N., and Lewis, S. A. (1997) Histone-induced damage of a mammalian epithelium: the role of protein and membrane structure. *Am. J. Physiol.* **273**, C1925–C1936

37. Kleine, T. J., Gladfelter, A., Lewis, P. N., and Lewis, S. A. (1995) Histone-induced damage of a mammalian epithelium: the conductive effect. *Am. J. Physiol.* **268**, C1114–C1125

38. Feng, Y., and Chao, W. (2011) Toll-like receptors and myocardial inflammation. *Int. J. Inflamm.* **2011**, 170352

39. Zhang, Y., Tocchetti, C. G., Krieg, T., and Moens, A. L. (2012) Oxidative and nitrosative stress in the maintenance of myocardial function. *Free Radic. Biol. Med.* **53**, 1531–1540

40. Santos, C. X., Anilkumar, N., Zhang, M., Brewer, A. C., and Shah, A. M. (2011) Redox signaling in cardiac myocytes. *Free Radic. Biol. Med.* **50**, 777–793

41. Zima, A. V., and Blatter, L. A. (2006) Redox regulation of cardiac calcium channels and transporters. *Cardiovasc. Res.* **71**, 310–321

42. Xu, K. Y., Zweier, J. L., and Becker, L. C. (1997) Hydroxyl radical inhibits sarcoplasmic reticulum Ca(2+)-ATPase function by direct attack on the ATP binding site. *Circ. Res.* **80**, 76–81

43. Giordano, F. J. (2005) Oxygen, oxidative stress, hypoxia, and heart failure. *J. Clin. Invest.* **115**, 500–508

44. Rudiger, A., and Singer, M. (2013) The heart in sepsis: from basic mechanisms to clinical management. *Curr. Vasc. Pharmacol.* **11**, 187–195

45. Hassoun, S. M., Marechal, X., Montaigne, D., Bouazza, Y., Decoster, B., Lancel, S., and Neviere, R. (2008) Prevention of endotoxin-induced sarcoplasmic reticulum calcium leak improves mitochondrial and myocardial dysfunction. *Crit. Care Med.* **36**, 2590–2596

46. Minamikawa, T., Sriratana, A., Williams, D. A., Bowser, D. N., Hill, J. S., and Nagley, P. (1999) Chloromethyl-X-rosamine (MitoTracker Red) photosensitises mitochondria and induces apoptosis in intact human cells. *J. Cell Sci.* **112**, 2419–2430

47. Knowlton, A. A., Chen, L., and Malik, Z. A. (2013) Heart Failure and Mitochondrial Dysfunction: The Role of Mitochondrial Fission/Fusion Abnormalities and New Therapeutic Strategies. *J. Cardiovasc. Pharmacol.*

48. Mignotte, B., and Vayssiere, J. L. (1998) Mitochondria and apoptosis. *Eur. J. Biochem* **252**, 1–15

49. Hanson, C. J., Bootman, M. D., and Roderick, H. L. (2004) Cell signalling: IP3 receptors channel calcium into cell death. *Curr. Biol.* **14**, R933–935

50. Takasu, O., Gaut, J. P., Watanabe, E., To, K., Fagley, R. E., Sato, B., Jarman, S., Efimov, I. R., Janks, D. L., Srivastava, A., Bhayani, S. B., Drewry, A., Swanson, P. E., and Hotchkiss, R. S. (2013) Mechanisms of cardiac and renal dysfunction in patients dying of sepsis. *Am. J. Respir. Crit. Care Med.* **187**, 509–517

51. Mekontso Dessap, A., Razazi, K., Brun-Buisson, C., and Deux, J. F. (2014) Myocardial viability in human septic heart. *Intensive Care Med.* **40**, 1746–1748

52. Oikonomopoulou, K., Ricklin, D., Ward, P. A., and Lambris, J. D. (2012) Interactions between coagulation and complement—their role in inflammation. *Semin. Immunopathol.* **34**, 151–165